

Evidence of shear-wave splitting in the eastern Corinthian Gulf (Greece)

P. Papadimitriou^{*}, G. Kaviris¹, K. Makropoulos²

Department of Geophysics, University of Athens, 157 84 Athens, Greece

Received 2 December 1997; accepted 2 November 1998

Abstract

The analysis of local earthquakes recorded by the Cornet network and located in the Gulf of Corinth (Greece) has revealed the existence of shear-wave splitting. The visual inspection technique is used to estimate the polarization direction of the fast shear wave and the time delay between the two split shear waves. The selected earthquakes are located close to one of the Cornet stations. Most of these earthquakes are recorded by only one station and their azimuth and angle of incidence are estimated using the covariance matrix decomposition method combined with the P-wave polarization direction. Polarigrams plotted for the horizontal components present a clear linear and almost constant polarization for each station, independent of the azimuth of the earthquake, except for one station where different S_{fast} polarization directions are observed. The mean direction of the fast shear wave polarization at Paradeisi station is 146°N , at Sofiko station 104°N and at Villia station 142°N . At Desfina station, two different main S_{fast} polarization directions were observed, one 143°N and the other 55°N . The calculated time delays between the two split shear waves are higher for the stations located in the eastern part of the Gulf. Comparing the mean S_{fast} polarization direction with the direction of local faulting, we observe that they are approximately parallel at Sofiko station, while at Villia station they are almost perpendicular. In general, the obtained mean S_{fast} polarization directions at the Cornet stations are perpendicular to the direction of the extension of the Gulf which is NNE–SSW and consistent with the extensive dilatancy anisotropy (EDA) model. © 1999 Elsevier Science B.V. All rights reserved.

Keywords: Shear-wave splitting; Seismic anisotropy; Cracks; Time delay

1. Introduction

Studies of local earthquakes performed worldwide have revealed the existence of shear-wave splitting in various sedimentary and crystalline geological

regimes (Crampin, 1978; Iannaccone and Deschamps, 1989; Kaneshima, 1990; Crampin and Lovell, 1991; Coutant, 1996; Gamar and Bernard, 1997). Since the beginning, the shear-wave splitting phenomenon has been related with the existence of anisotropic medium. When an approximately vertical shear wave propagates through effectively anisotropic media, it splits into two components: the S_{fast} and the S_{slow} . These two shear waves have different arrival times and nearly orthogonal polarizations.

^{*} Corresponding author. Fax: +30-1-7243217; e-mail: ppapadim@geol.uoa.gr

¹ Fax: +30-1-7243217; e-mail: gkaviris@geol.uoa.gr.

² Fax: +30-1-7243217; e-mail: kmacrop@geol.uoa.gr.

The observed time delay between the two split shear waves defines the magnitude of anisotropy and is related to the crack density, the crack aspect ratio and the length of the ray path in the anisotropic medium.

Various models have been proposed to explain the observed seismic anisotropy: crystalline anisotropy based on aligned anisotropic crystals (Babuska, 1984), lithological anisotropy based on aligned non-spherical sediment grains (Crampin et al., 1984a), PTL anisotropy that is based on periodic thin layering of isotropic materials (Postma, 1955; Levin, 1978; Helbig, 1984) and extensive dilatancy anisotropy (EDA) based on aligned cracks and microcracks (Crampin, 1978). Many authors have interpreted crustal anisotropy in terms of cracks in many different geological and tectonic environments. Crampin et al. (1984b) and Crampin (1993) suggest that cracks, fractures and pore spaces will preferentially align with the current stress field, parallel to the maximum horizontal compressive stress. In some cases the polarization direction of the S_{fast} wave is not in agreement with the regional compressive stress (Savage et al., 1989; Kaneshima, 1990). Other models were proposed in order to explain this fact, such as microcracks reflecting a paleostress (Blenkinsop, 1990; Sachpazi and Hirn, 1991) or intrinsic anisotropy

caused by rock fabric (Kern and Wenk, 1990). Another possible explanation is the preferential crystal orientation model. In this model, the solid is homogeneously and continuously anisotropic down to its smallest particle size (Brocher and Christensen, 1990; Aster and Shearer, 1992). Zatsepin and Crampin (1995) proposed the anisotropic poroelasticity (APE) model based on the effects of stress on fluid-saturated cracked rock. The temporal changes in the time delays between split shear waves, which were observed, are successfully explained by the APE model (Crampin and Zatsepin, 1997; Liu et al., 1997). Vertically oriented microcracks, parallel to active faults, may also be responsible for shear-wave splitting (Gledhill, 1991; Zhang and Schwartz, 1994; Evans et al., 1995). In some cases, more than one of the above mentioned models may contribute simultaneously to the observed anisotropy directions.

In this paper, we present evidence for the existence of shear-wave anisotropy in the Corinthian Gulf (Greece) using short-period recordings of local earthquakes. It is important to estimate the anisotropy as it is related to the strain field of the medium and therefore to geodynamics. The correction of the observed anisotropy is also important in order to recover the polarization information due to the source (Zollo and Bernard, 1989).

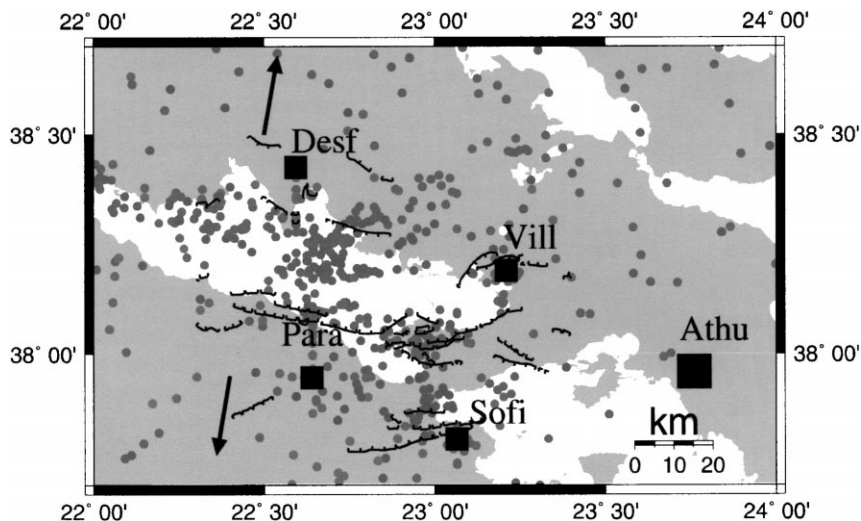


Fig. 1. Active normal faults of the area and epicenters located by Cornet network. The arrows present the extension of the Gulf of Corinth.

2. Data acquisition and methodology

The Cornet seismological permanent network has been installed since 1995 around the eastern Gulf of Corinth (Greece), which is an area characterized by high seismic activity (Papadimitriou et al., 1996). This network consists of five digital telemetric Lennartz stations with L4 and Le-3D (1 Hz) seismometers, recording with a sampling rate of 125 samples/s. More than 1500 earthquakes were recorded by the Cornet network during 1996 with magnitudes less than 4.0 (M_L) and hypocentral depths located in the crust. Fig. 1 shows the best located earthquakes for this period using HYPO71

program (Lee and Lahr, 1975). More than 300 earthquakes are well located within the network.

The shear-wave splitting phenomenon has been observed during the analysis of the Cornet data set. The data set used in this study is comprised of 126 microearthquakes, 36 of which were located using HYPO71 program and 90 were recorded by only one station. All these events are located close to one of the Cornet stations and were selected to have incident angles smaller than the critical angle in order to avoid the S to P converted phases (Booth and Crampin, 1985). The selected events have clear and impulsive S-wave arrival phases on the horizontal components. In addition the amplitude of the S-wave

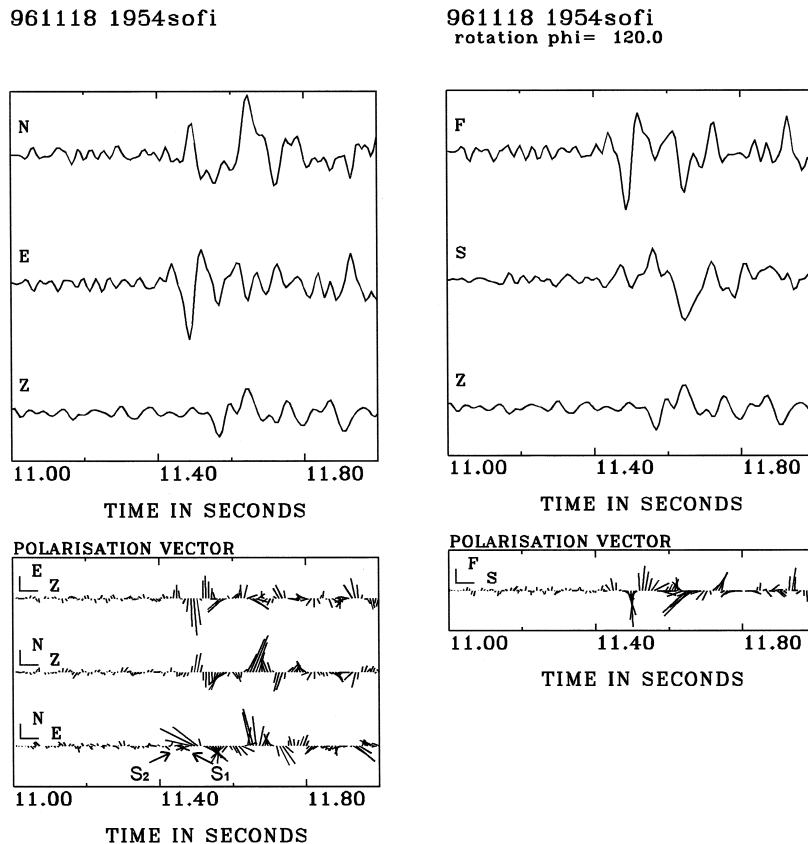


Fig. 2. (a) Three component seismograms of an earthquake recorded at Sofiko station. The original traces are presented at the top of the figure. At the bottom the polarization vector is presented in the east-up, north-up and north-east planes, respectively. The vector is oriented almost parallel to the horizontal components. In the north-east plane the polarization directions of the fast (S_1) and the slow (S_2) shear waves are indicated. (b) The original seismograms of (a) are rotated parallel and orthogonal to the polarization direction of the fast shear waves and the obtained waveforms are presented at the top of the figure. At the bottom, the polarization vector is presented in the fast-slow plane where the time delay is measured.

phase on the vertical component is smaller than on the horizontal ones.

A visual inspection and a plot of the particle motion in the three planes of projection were used to select the events that match the criteria mentioned above. Some of the selected recordings were filtered using a band-pass filter in the frequency range of 1 to 15 Hz in order to obtain a better representation of the waveform. The representation used in the present study in order to determine the polarization direction of the S_{fast} and the time delay between the two split shear waves is the polarization vector as a function of time (polarigram), as proposed by Bernard and Zollo (1989). Fig. 2 shows an example of an event

located close to the Sofiko station, where the components E–Z and N–Z are plotted. It is evident that the polarization vector is oriented almost parallel to the horizontal component (east and north, respectively), showing that the vertical component has smaller amplitudes than the horizontal ones. This fact indicates that the shear waves are propagating approximately vertically through the anisotropic media.

In the same figure, the polarigram of the north–east plane is also presented. In this representation, the shear-wave splitting is evident. The angle between the north and the fast axis direction is the polarization direction, which is equal to 120°N . Then, the seismograms are rotated in the fast and slow

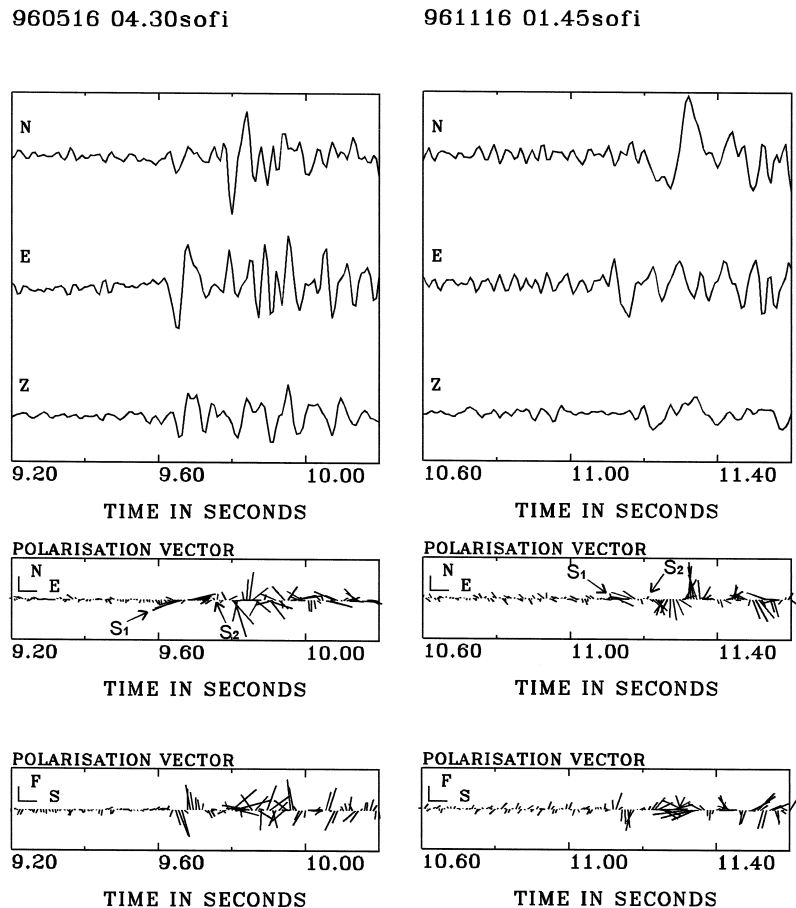


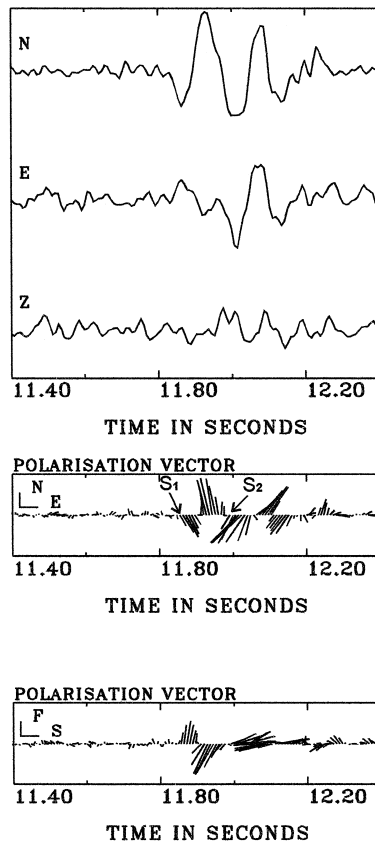
Fig. 3. (a) Three component seismograms of an earthquake recorded at Sofiko station. The original traces are presented at the top of the figure. In the middle the polarization vector is presented in the north–east plane where the polarization directions of the fast and the slow shear waves are indicated. At the bottom, the polarization vector of the rotated waveforms is presented in the fast–slow plane where the time delay is measured. (b) Same as (a) for another earthquake with different polarization direction of the fast shear wave.

direction and the obtained polarigram is presented in Fig. 2b. In this figure, the obtained polarization vector is oriented almost parallel to the fast component. The measured time delay is equal to 0.040 s, represents the magnitude of the anisotropy and is removed in order to obtain the polarization direction of the source. In cases where the direction of the fast axis was not clear in the polarigram, the hodogram representation was also used.

The Cornet network has also recorded numerous microearthquakes in only one station where the shear-wave splitting is also evident. The azimuth and the angle of incidence for these events were esti-

mated using the methodology of Kanasevich (1981) for the first P-wave window, as well as the polarization of the first P-wave motion recorded in the three components. The Kanasevich method is based on the covariance matrix decomposition where the eigenvalues were calculated by diagonalization of the matrix. By the calculation of the eigenvector that corresponds to the maximum eigenvalue, we can evaluate the angle of incidence and the azimuth. Nevertheless, the results obtained by the above method depend on the selection of the P-wave window and, therefore, they are not always reliable. For that reason all the values of the azimuth and of the

960430 00.19para



970203 21.27para

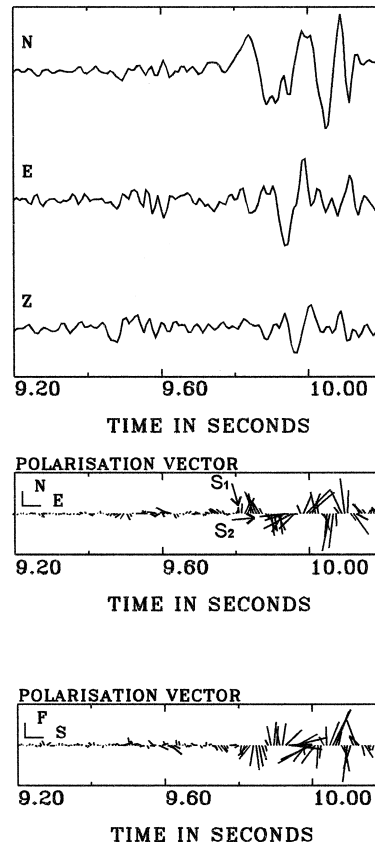


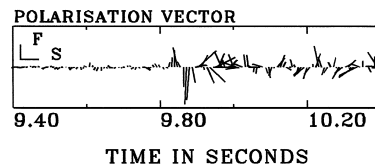
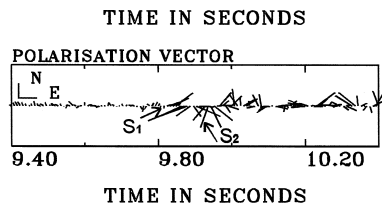
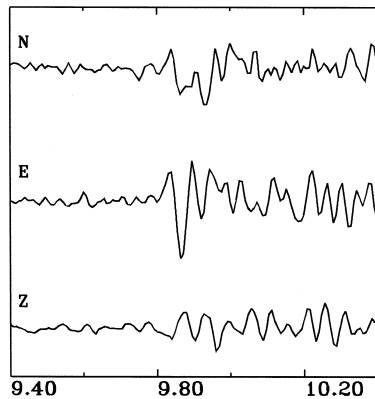
Fig. 4. (a) Three component seismograms of an earthquake recorded at Paradeisi station. The original traces are presented at the top of the figure. In the middle the polarization vector is presented in the north–east plane where the polarization directions of the fast and the slow shear waves are indicated. At the bottom, the polarization vector of the rotated waveforms is presented in the fast–slow plane where the time delay is measured. (b) Same as (a) for another earthquake with different polarization direction of the fast shear wave.

angle of incidence were compared with the ones obtained by the P-wave polarization. This comparison showed that even though the P-wave polarization was often unstable in the beginning of the first motion, it was consistent with the values obtained by the Kanasewich method close to the maximum of the first P-wave motion. In this study, we only used the events that had similar results from both methods. Only 5% of the initially selected events were rejected.

Bouin et al. (1996) performed a study on the western Corinthian Gulf, using the Kanasewich technique for the measurement of the direction of the fast S-wave polarization. Aster et al. (1990) used an

automatic method to measure the fast S-wave polarization but Liu et al. (1997) claim that this method introduced significant errors in time delays and that there is no automatic technique that can reliably measure shear-wave splitting above local earthquakes. The measurement of the time delay between the two split shear waves can also be obtained using the classical cross-correlation method (Bowman and Ando, 1987; Papadimitriou et al., 1993; Zhang and Schwartz, 1994). This method was used in some cases in this study, but the results were not always reliable. For these reasons, in this study we essentially used the standard visual method mentioned above.

960106 16.22desf



970118 03.07desf

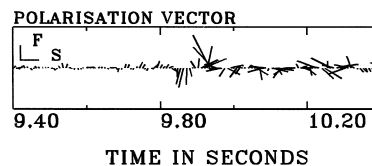
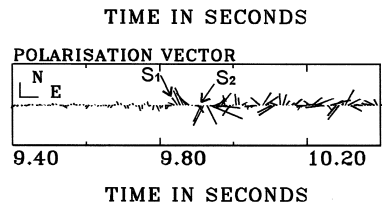
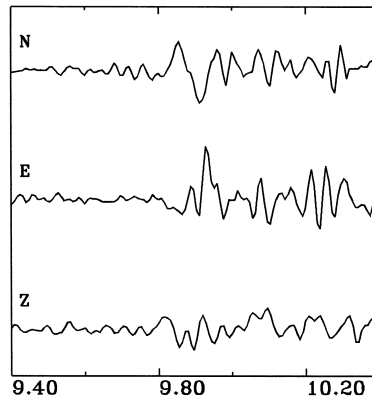


Fig. 5. (a) Three component seismograms of an earthquake recorded at Desfina station. The original traces are presented at the top of the figure. In the middle the polarization vector is presented in the north–east plane where the polarization directions of the fast and the slow shear waves are indicated. At the bottom, the polarization vector of the rotated waveforms is presented in the fast–slow plane where the time delay is measured. (b) Same as (a) for another earthquake with different polarization direction of the fast shear wave.

3. Results

In this study, the selected local earthquakes are located close to one of the stations of the Cornet network in order to fulfill the selection criteria. Events recorded by only one station were also used. Their magnitudes are $M_L \leq 2.6$ and the depth variation is between surface and 29 km. In general, the recorded events in the Gulf of Corinth and the surrounding areas show evidence for the existence of shear-wave splitting. Using the methodology mentioned above, we present the results of the shear wave polarization directions that refer to the Sofiko, Paradeisi, Desfina and Villia stations, respectively.

Fig. 3a and b present two typical earthquakes recorded by the Sofiko station where no filter was used, as the shear-wave splitting was evident. For the first event (Fig. 3a), the orientation of the S_{fast} is $88^\circ N$ and the time delay is $dt = 0.128$ s. The S_{fast} polarization direction in the second event (Fig. 3b) is $95^\circ N$ and the time delay is $dt = 0.144$ s. In both examples, the direction of anisotropy is approximately east–west and the calculated values of the time delays are high. Another set of earthquakes recorded in Sofiko indicates an anisotropy direction close to $120^\circ N$ (Fig. 2a).

The same procedure is followed for the Paradeisi station where two typical examples are shown

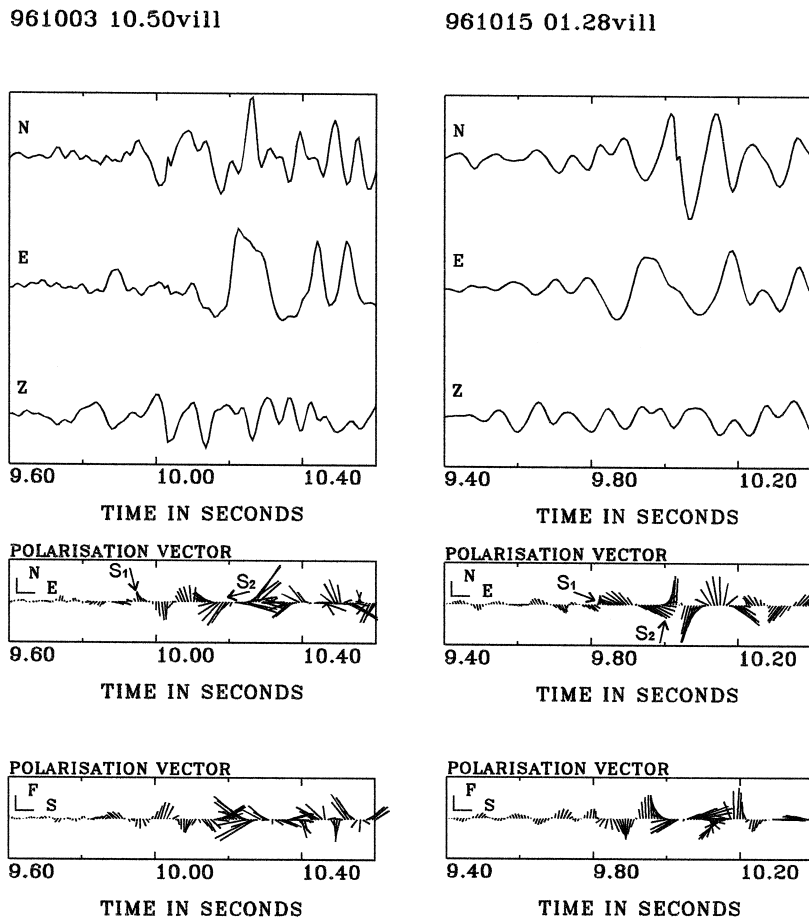


Fig. 6. (a) Three component seismograms of an earthquake recorded at Villia station. The original traces are presented at the top of the figure. In the middle the polarization vector is presented in the north–east plane where the polarization directions of the fast and the slow shear waves are indicated. At the bottom, the polarization vector of the rotated waveforms is presented in the fast–slow plane where the time delay is measured. (b) Same as (a) for another earthquake with different polarization direction of the fast shear wave.

(Fig. 4a and b). The measured S_{fast} polarization direction of the event presented in Fig. 4a is 140°N , while the one of the second event (Fig. 4b) is 165°N . In order to estimate the time delay, the waveforms of each event are rotated to their respective S_{fast} polarization direction. Both events present a time delay between the two split shear waves $dt = 0.080$ s. These two directions are the main axes of anisotropy observed in the Paradeisi station.

The most complicated site is Desfina station where various S_{fast} polarization directions are observed. Nevertheless, there are two dominant directions. The first one is between 20°N and 90°N and the second between 135°N and 160°N . In Fig. 5a and b, two representative examples are presented with S_{fast} directions 65°N and 140°N , respectively. These two directions are almost orthogonal. The time delay of the first event is $dt = 0.072$ s and of the second $dt = 0.024$ s. Finally, two earthquakes recorded by the Villia station are presented in Fig. 6a and b. The S_{fast} polarization direction of the first example (Fig. 6a) is 156°N and the calculated time delay is $dt = 0.136$ s. In the second example (Fig. 6b) the S_{fast} polarization direction is 125°N and the time delay is $dt = 0.176$ s.

Fig. 7 presents the S_{fast} polarization directions on equal-area projections of the upper hemisphere for each station. The outer circle defines the S-wave window and represents an angle of incidence of 45° . The selected events are both located earthquakes and events recorded by only one station. The azimuth and the angle of incidence of each event are estimated using the Kanasewich methodology and the P-wave polarization. The length of the bars is proportional to the time delay between the fast and slow shear waves. The values of the time delays at Sofiko station vary between 0.024 and 0.152 s, while the polarization directions of the fast shear wave vary between 78°N and 126°N . The coherence of the fast shear wave polarizations at Sofiko station, irrespective of the azimuth of each event, is consistent with shear-wave splitting due to the seismic wave propagation through an anisotropic medium. The same observation is evident for the Paradeisi and Villia stations. The values of the time delays at Paradeisi station vary between 0.024 and 0.096 s, while at Villia station between 0.040 and 0.184 s. The polarization directions of the fast shear wave at Paradeisi

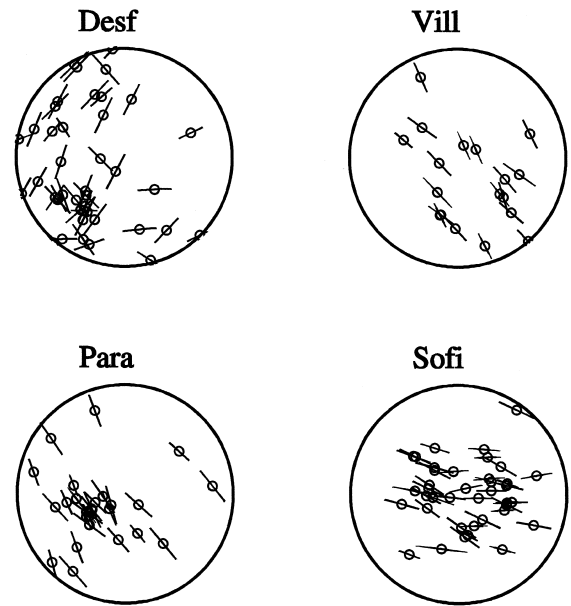


Fig. 7. Polar equal-area projections on the upper hemisphere of the fast shear wave polarizations measured at each station for both located and unlocated events. The length of the bars is proportional to the time delay of each event and the circle represents an angle of incidence equal to 45° .

station vary between 125°N and 165°N , while at Villia station between 125°N and 163°N . Desfina station gives more complicated results as the shear wave polarizations present two different and quasi-perpendicular main directions. The values of the time delays at Desfina station vary between 0.024 and 0.096 s, while the polarization directions of the fast shear wave vary between 20°N and 160°N . Comparing the calculated time delays, we observe that they have higher values in the stations situated in the eastern part of the Gulf (Sofiko and Villia).

The S_{fast} polarization directions at each station are presented in Fig. 8 using equal-area rose diagrams. The mean direction at Sofiko station is 104°N . At Paradeisi station, we observe two directions of anisotropy with a mean value equal to 146°N , while at Villia station there are three directions with a mean value equal to 142°N . Finally, at Desfina station various directions of anisotropy are observed. However, two main directions can be distinguished, one approximately 55°N and the second 143°N .

The mean values of the anisotropy direction of each station are presented in Fig. 9. The mean

polarization directions at Paradeisi, Villia and Desfina (one of the two main directions) stations are very similar, close to 145°N , while the one measured at Sofiko station is more east–west. These observations are consistent with the general NNE–SSW direction of extension of the Gulf of Corinth and, therefore, in agreement with the EDA model. The second mean polarization direction (55°N) observed in Desfina station differs significantly from the orientation of the maximum compressive axis calculated above. Bouin et al. (1996) also detected in the western part of the Gulf of Corinth two main directions of fast S-wave polarization: one oriented 105°N – 120°N , the other 55°N – 75°N which are similar to the results of our study. Karnassopoulou (1996) also measured two different S_{fast} polarization directions at the same site, in Almiros area (Central Greece). One of these directions was in agreement with the main direction of extension of the area, while the second one was attributed to the local stress field. The possibility of the presence of two anisotropic layers of different properties or of one in which there are microcracks oriented in two different directions could explain the observation of different S_{fast} polarization directions at Desfina station. Another explanation of this discrepancy could be that the first mean direction (143°N) is in agreement with the extension of the Corinthian Gulf, while the second one (55°N) is due to the rotation of the direction

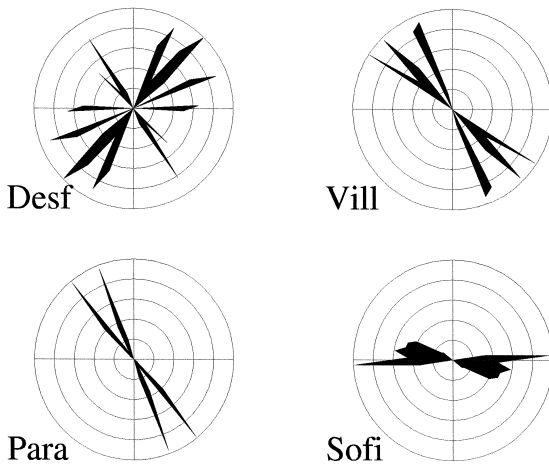


Fig. 8. Rose diagrams of the fast shear wave polarization directions at all the sites.

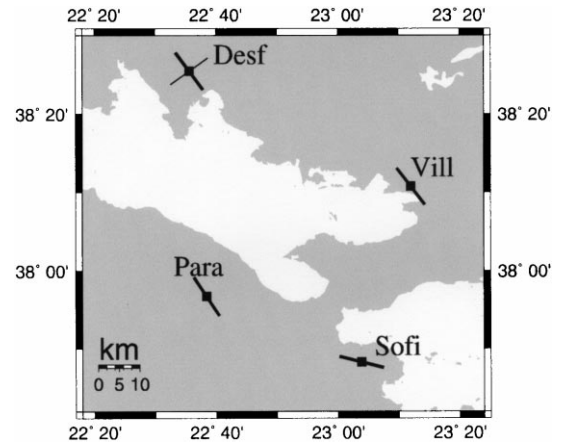


Fig. 9. Mean S_{fast} polarization directions at the Cornet stations. The thick bars centered at each station represent the directions that are consistent with the extension of the Gulf and the thin one is the second mean S_{fast} polarization direction calculated at Desfina station.

of stress caused by active local faults. It should be noted that most of the selected recordings of Desfina station have not been recorded by the other Cornet stations and this fact imposes limitations to the interpretation of the results.

4. Discussion

The analysis of the data recorded by the Cornet network revealed the existence of an anisotropic upper crust around the Gulf of Corinth. Shear-wave splitting was observed for the majority of the recorded events (more than 300). Most of the events located in the Gulf exhibit shear-wave splitting, but they do not fulfill the selection criteria. The Gulf of Corinth is an area characterized by normal faulting (Fig. 1) and a NNE–SSW direction of extension (Jackson et al., 1982; Papadimitriou et al., 1994; Hatzfeld et al., 1996; Rigo et al., 1996). The polarization directions calculated at Paradeisi and Sofiko stations are almost perpendicular to this direction of extension. In this case, the observed shear-wave splitting can be explained by the existence of fluid-filled cracks preferentially oriented parallel to the local maximum horizontal compressive stress of the area. Shear waves traveling through these cracks split into two orthogo-

nal components and the fast component is polarized parallel to the orientation of the cracks. This explanation is consistent to the EDA model.

The directions of polarization calculated at Desfina station are the most complicated ones. Two different main directions were observed. The first one is approximately the same (143°N) with the main direction observed at the other stations. The second direction (55°N) is almost perpendicular to the first one and is differentiated with the stress field of the area. This direction has also been observed at different sites western of Desfina station and has been explained by the existence of active local faults that rotate the direction of stress (Bouin et al., 1996). The results of our study provoke further investigation in order to explain the observation of different polarization directions at Desfina station, as several different models (mentioned above) could explain this observation.

The mean S_{fast} polarization direction that is calculated at Villia station is in agreement with the ones observed at the southern stations of the network (Sofiko and Paradeisi). This direction is differentiated from the direction of the observed surface faults of the area, which is approximately E–W (Jackson et al., 1982), but it is still in agreement with the stress field of the region. On the other hand, the mean polarization direction measured at Sofiko station is in agreement with the observed surface faults of the area. In general, the EDA model can explain the crack anisotropy distributions in the eastern part of the Gulf of Corinth.

Acknowledgements

We thank Aphrodite Karnassopoulou for her comments on this manuscript. This project was supported by the European Commission through contract numbers ENV-CT96-0276 and ENV-CT96-0277.

References

- Aster, R.C., Shearer, P.M., 1992. Initial particle motions and stress constraints at the Anza seismic network. *Geophys. J. Int.* 108, 1–9.
- Aster, R.C., Shearer, P., Berger, J., 1990. Quantitative measurements of shear-wave polarization at the Anza seismic network, southern California: implications for shear-wave splitting and earthquake prediction. *J. Geophys. Res.* 95, 12449–12473.
- Babuska, V., 1984. P-wave velocity anisotropy in crystalline rocks. *Geophys. J. R. Astron. Soc.* 76, 113–119.
- Bernard, P., Zollo, A., 1989. Inversion of near-source S polarization for parameters of double-couple point like sources. *Bull. Seismol. Soc. Am.* 79, 1779–1809.
- Blenkinsop, T.G., 1990. Correlation of paleotectonic fracture and microfracture orientations in cores with seismic anisotropy at Cajon Pass drill hole, southern California. *J. Geophys. Res.* 95, 11143–11150.
- Booth, D.C., Crampin, S., 1985. Shear wave polarizations on a curved wavefront at an isotropic free surface. *Geophys. J. R. Astron. Soc.* 83, 61–73.
- Bouin, M.P., Tellez, J., Bernard, P., 1996. Seismic anisotropy around the Gulf of Corinth, Greece, deduced from three-component seismograms of local earthquakes and its relationship with crustal strain. *J. Geophys. Res.* 101, 5797–5811.
- Bowman, J.R., Ando, M., 1987. Shear-wave splitting in the upper mantle wedge above the Tonga subduction zone. *Geophys. J. R. Astron. Soc.* 88, 25–41.
- Brocher, T.M., Christensen, N.I., 1990. Seismic anisotropy due to preferred mineral orientation observed in shallow crustal rocks in southern Alaska. *Geology* 18, 737–740.
- Coutant, O., 1996. Observation of shallow anisotropy on local earthquake records at the Garner Valley, southern California, downhole array. *Bull. Seismol. Soc. Am.* 86, 477–488.
- Crampin, S., 1978. Seismic-waves propagating through a cracked solid: polarization as a possible dilatancy diagnostic. *Geophys. J. R. Astron. Soc.* 53, 467–496.
- Crampin, S., 1993. Arguments for EDA. *Can. J. Exp. Geophys.* 29, 3–17.
- Crampin, S., Lovell, H.L., 1991. A decade of shear-wave splitting in the Earth's crust: what does it mean? what can we make of it? and what should we do next?. *Geophys. J. Int.* 107, 387–407.
- Crampin, S., Zatsepina, S.V., 1997. Changes of strain before earthquakes: the possibility of routine monitoring of both long-term and short-term precursors. *J. Phys. Earth* 45, 1–26.
- Crampin, S., Chesnokov, E.M., Atkinson, B.K., 1984a. Seismic anisotropy—the state of the art: II. *Geophys. J. R. Astron. Soc.* 76, 1–16.
- Crampin, S., Evans, J.R., Atkinson, B.K., 1984b. Earthquake prediction: a new physical basis. *Geophys. J. R. Astron. Soc.* 76, 147–156.
- Evans, J.R., Julian, B.R., Foulger, G.R., Ross, A., 1995. Shear wave splitting from local earthquakes at the Geysers geothermal fields California. *Geophys. Res. Lett.* 22, 501–504.
- Gamar, F., Bernard, P., 1997. Shear wave anisotropy in the Erzincan basin and its relationship with crustal strain. *J. Geophys. Res.* 102, 20373–20393.
- Gledhill, K.R., 1991. Evidence for shallow and pervasive seismic anisotropy in the Wellington region New Zealand. *J. Geophys. Res.* 96, 21503–21516.
- Hatzfeld, D., Kementzetzidou, D., Karakostas, V., Ziazia, M., Nothard, S., Diagourtas, D., Deschamps, A., Karakaisis, G.,

- Papadimitriou, P., Scordilis, M., Smith, R., Voulgaris, N., Kiratzi, S., Makropoulos, K., Bouin, M.P., Bernard, P., 1996. The Galaxidi earthquake of November 18, 1992: a possible asperity within the normal fault system of the Gulf of Corinth (Greece). *Bull. Seismol. Soc. Am.* 86 (6), 1987–1991.
- Helbig, K., 1984. Anisotropy and dispersion in periodically layered media. *Geophysics* 49, 364–373.
- Iannaccone, G., Deschamps, A., 1989. Evidence of shear wave anisotropy in the upper crust of central Italy. *Bull. Seismol. Soc. Am.* 76, 1905–1912.
- Jackson, J.J., Gagnepain, J., Houseman, G., King, G., Papadimitriou, P., Soufleris, P., Virieux, J., 1982. Seismicity, normal faulting and the geomorphological development of the Gulf of Corinth (Greece): the Corinth earthquakes of February and March 1981. *Earth Planet. Sci. Lett.* 57, 377–397.
- Kanasewich, E.R., 1981. *Time Sequence Analysis in Geophysics*. Univ. of Alberta Press, Edmonton, Alberta.
- Kaneshima, S., 1990. Origin of crustal anisotropy: shear wave splitting studies in Japan. *J. Geophys. Res.* 95, 11121–11133.
- Karnassopoulou, A., 1996. Joint investigation of source parameters and seismic anisotropy using microearthquakes in Greece, Arkansas and Northeast Brazil. PhD thesis, University of Edinburgh.
- Kern, H., Wenk, H.R., 1990. Fabric-related velocity anisotropy and shear wave splitting in rocks from the Santa Rosa mylonite zone California. *J. Geophys. Res.* 95, 11213–11224.
- Lee, W.H.K., Lahr, J.C., 1975. HYPO71 (revised): a computer program used for determining hypocenter, magnitude and first motion pattern of local earthquakes. *US Geol. Surv., Open-File Rep.* 114, 75–311.
- Levin, F.K., 1978. The reflection, refraction and diffraction of waves in media with elliptic velocity dependence. *Geophysics* 43, 528–537.
- Liu, Y., Crampin, S., Main, I., 1997. Shear-wave anisotropy: spatial and temporal variations in time delays at Parkfield Central California. *Geophys. J. Int.* 130, 771–785.
- Papadimitriou, P., Makropoulos, K., Drakopoulos, J., 1993. Shear-wave splitting and earthquake prediction. Proceedings of the 2nd congress of the Hellenic Geophysical Union. Florina, Greece.
- Papadimitriou, P., Kassaras, I., Rigo, A., Lyon-Caen, H., Hatzfeld, D., Makropoulos, K., Drakopoulos, J., 1994. Source parameters of large and small earthquakes in Corinth Gulf (C. Greece). Proceedings of the XXIV General Assembly of ESC, Vol. II, Athens, Greece, pp. 848–858.
- Papadimitriou, P., Makropoulos, K., Kassaras, I., Kaviris, G., Drakopoulos, J., 1996. The eastern Corinthian Gulf (Greece) seismological telemetry network (Cornet). XXV General Assembly of ESC, Reykjavik, Iceland.
- Postma, G.W., 1955. Wave propagation in a stratified medium. *Geophysics* 20, 780–806.
- Rigo, A., Lyon-Caen, H., Armijo, R., Deschamps, A., Hatzfeld, D., Makropoulos, K., Papadimitriou, P., Kassaras, I., 1996. A microseismic study in the western part of the Gulf of Corinth (Greece): implications for large-scale normal faulting mechanisms. *Geophys. J. Int.* 126, 663–688.
- Sachpazi, M., Hirn, A., 1991. Shear-wave anisotropy across the geothermal field of Milos, Aegean Volcanic arc. *Geophys. J. Int.* 114, 759–777.
- Savage, M.K., Shih, X.R., Meyer, R.P., Aster, R., 1989. Shear-wave anisotropy of active tectonic regions via automated S wave polarization analysis. *Tectonophysics* 165, 279–292.
- Zatsepin, S.V., Crampin, S., 1995. The metastable poro-reactive and interactive rockmass: anisotropic poro-elasticity. 65th Ann. Int. SEG Meeting, Houston, Expanded Abstracts, pp. 918–921.
- Zhang, Z., Schwartz, S.Y., 1994. Seismic anisotropy in the shallow crust of the Loma Prieta segment of the San Andreas fault system. *J. Geophys. Res.* 99, 9651–9661.
- Zollo, A., Bernard, P., 1989. S-wave polarization inversion of the October 1979, 23:19 Imperial Valley aftershock: evidence for anisotropy and a simple source mechanism. *Geophys. Res. Lett.* 16, 1047–1050.